14 Interference zones, plane waves

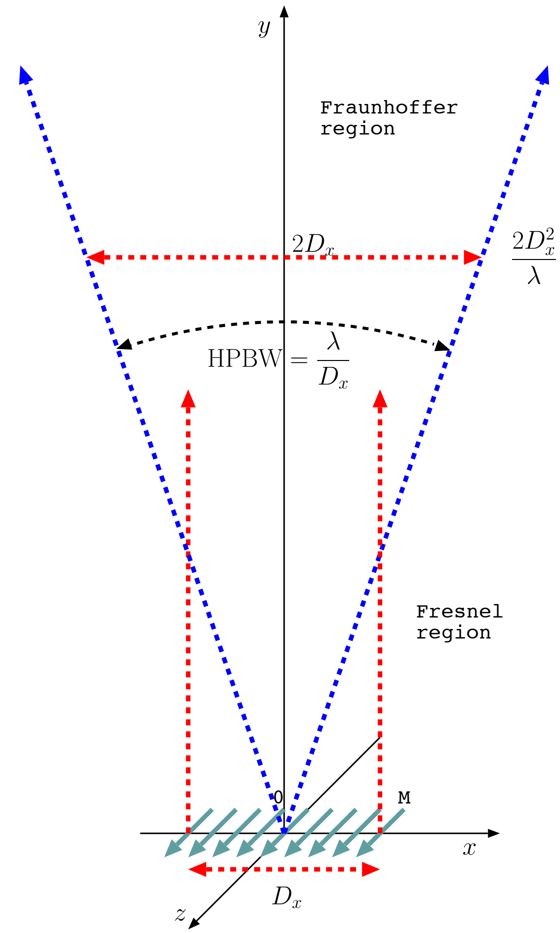

- Let's examine the radiation field of a 1D array of $N = 2M + 1$ identical elements located at $(nd, 0, 0)$, with n in the interval $-M, \cdots -1, 0, 1, \cdots M$ having *spherical* wave field phasors

$$\tilde{\mathbf{E}}_n(\mathbf{r}) = j\eta_o I_n k\ell \sin\theta_n \frac{e^{-jk|\mathbf{r}-\hat{x}nd|}}{4\pi|\mathbf{r}-\hat{x}nd|}\hat{\theta}_n$$

  where

$$\cos\theta_n = \hat{z} \cdot \frac{\mathbf{r}-\hat{x}nd}{|\mathbf{r}-\hat{x}nd|}.$$

- The total field phasor

$$\tilde{\mathbf{E}}(\mathbf{r}) = \sum_{n=-M}^{M} \tilde{\mathbf{E}}_n(\mathbf{r})$$

  of the array will have different types of spatial variations in different *interference zones* or *regions*:

1. The region

$$|\mathbf{r}| \lesssim \frac{2D_x^2}{\lambda}, \text{ where } D_x = 2Md$$

   is the physical length of the array, is known as **Fresnel region** or the **near-field** radiation zone — in this zone paraxial approximation cannot be used and the radiation field is highly structured having a prominent magnitude directly above the array (i.e., for $-Md \lesssim x \lesssim Md$).

2. The region

$$|\mathbf{r}| \gtrsim \frac{2D_x^2}{\lambda}$$

is known as **Fraunhoffer region** or the **far field** — this is the zone in which paraxial approximation works well, and spherical waves arriving from individual array elements merge to become a single spherical wave of a higher directivity.

The concept of *antenna beam* applies only in the Fraunhoffer region. A beam with a fixed angular width emerges out of the Fresnel region as Fraunhoffer region is approached, as shown in the cartoon in the margin (in which an "unphased" broadside array has been assumed in sketching the far-field beam).

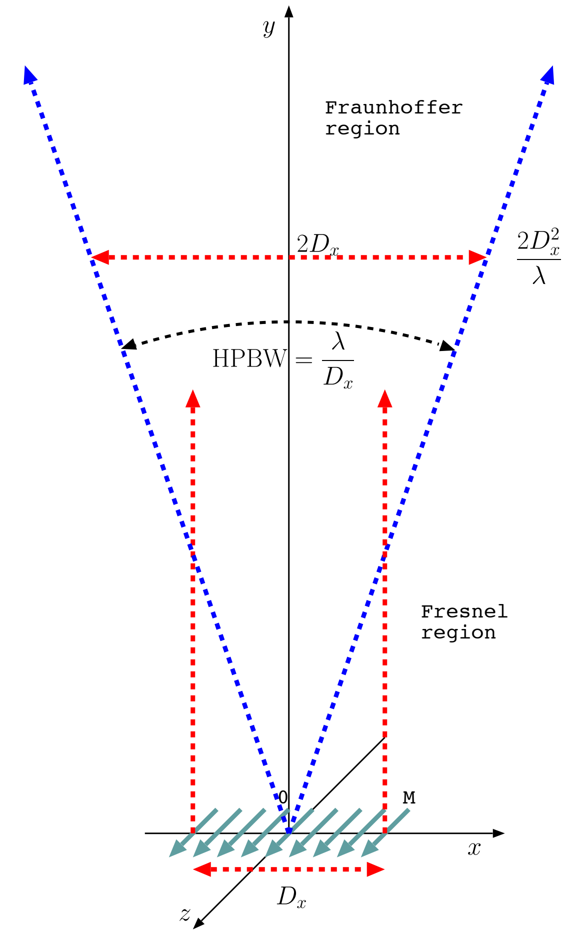

- In addition, it should be noted that
  - the region $|\mathbf{r}| \lesssim$ few λ will include strong storage fields, whereas
  - for $|\mathbf{r}| \gg \frac{2D_x^2}{\lambda}$, deep in Fraunhoffer region, spherical waves will "locally" look like plane waves.

We will next examine the transition between Fresnel and Fraunhoffer regions and then examine how spherical waves can be treated as plane waves over limited regions of space in the far-field.

- Consider the "phase-delay" of signals arriving from individual elements of a broadside array on the x-axis to a location $(0, r, 0)$ on the y-axis as shown in the margin.

  - Clearly, the sample "rays" shown in the margin connecting different array elements to $(0, r, 0)$ have different lengths even though in *paraxial approximation* only one length, r, would be assigned to all them since $nd\cos\theta_x = 0$ for $\theta_x = 90°$.

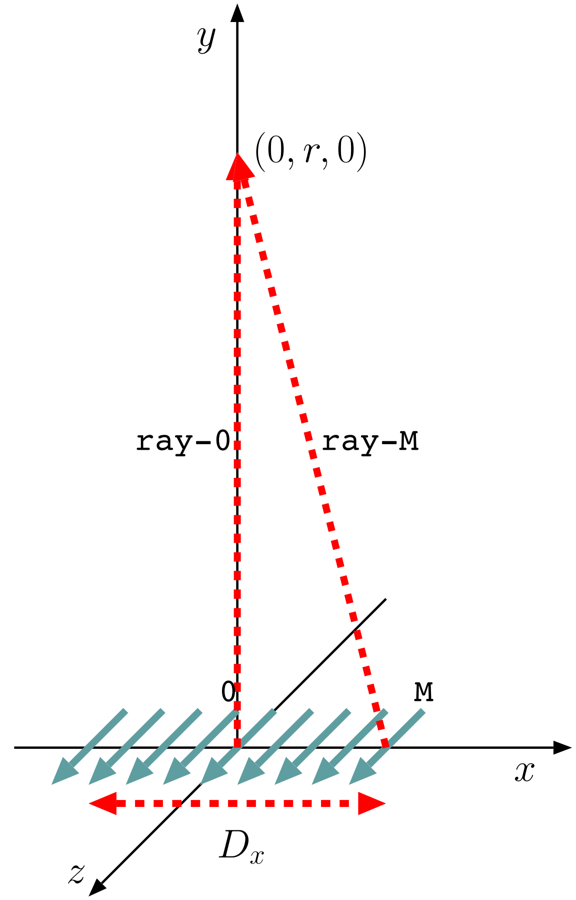

This discrepancy between r and the *actual* ray length $|r\hat{y} - nd\hat{x}|$ would be the cause of the failure of paraxial approximation, except when the "phase error" caused by the discrepancy is *unimportant* (because it is small in radian units).

  - The exact phase delay along ray-0 is

$$\Phi_0 = kr$$

    since the field phasor arriving along this path from element $n = 0$ is $\propto e^{-jkr}$.

  - The exact phase delay along ray-M is

$$\Phi_M = k|r\hat{y} - Md\hat{x}| = k|r\hat{y} - \frac{D_x}{2}\hat{x}| = k\sqrt{r^2 + (\frac{D_x}{2})^2}$$

    since the field phasor arriving along this path from element $n = M$ is $\propto e^{-jk|r\hat{z} - Md\hat{x}|}$.

– The maximum phase error made in paraxial approximation is then

$$\begin{aligned}\Delta\Phi &= \Phi_M - \Phi_0 = k\sqrt{r^2 + (\frac{D_x}{2})^2} - kr = k(\sqrt{r^2 + (\frac{D_x}{2})^2} - r) \\ &= kr(\sqrt{1 + (\frac{D_x}{2r})^2} - 1).\end{aligned}$$

Note that this phase error vanishes when $r \to \infty$. But for a finite r, we have, when $r \gg \frac{D_x}{2}$, a finite error of about

$$\begin{aligned}\Delta\Phi &= kr(\sqrt{1 + (\frac{D_x}{2r})^2} - 1) \\ &\approx kr(1 + \frac{1}{2}(\frac{D_x}{2r})^2 - 1) = \frac{2\pi}{\lambda}\frac{D_x^2}{8r} = \frac{\pi}{8}\frac{2D_x^2}{\lambda r},\end{aligned}$$

using the first two terms of the binomial expansion of $\sqrt{1 + (\frac{D_x}{2r})^2}$.

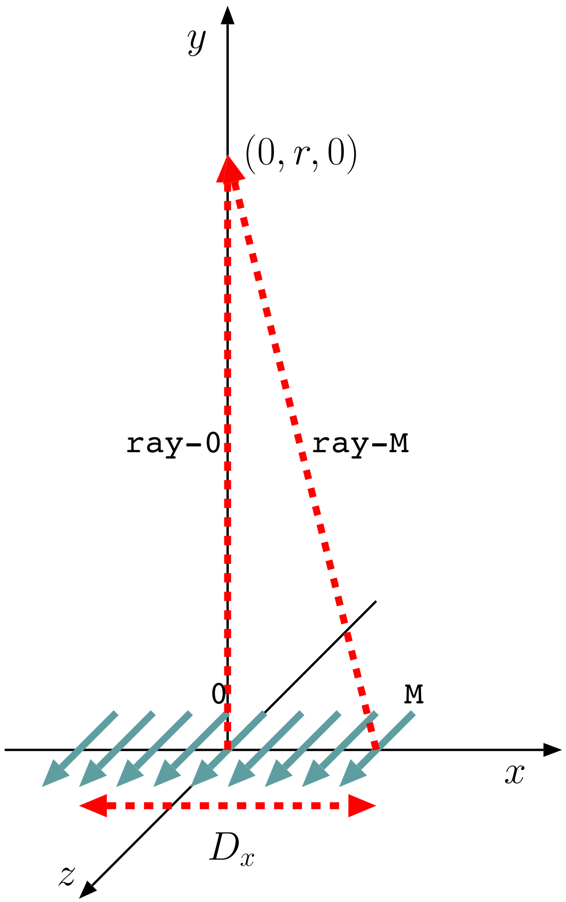

– Clearly then, if we were to take

$$\frac{2D_x^2}{\lambda r} \lesssim 1 \quad \Leftrightarrow \quad r \gtrsim \frac{2D_x^2}{\lambda} \text{ then we would have } \Delta\Phi \lesssim \frac{\pi}{8} \text{ rad},$$

which is a small enough of a phase error that can actually be neglected (in particular in multiple-element arrays where the phase errors due to a multitude of other elements will be even smaller than $\frac{\pi}{8}$ rad or 22.5°).

The analysis just concluded indicates that the border between Fresnel and Fraunhoffer zones can be taken as

$$r \sim \frac{2D_x^2}{\lambda},$$

the so-called *Rayleigh distance*.

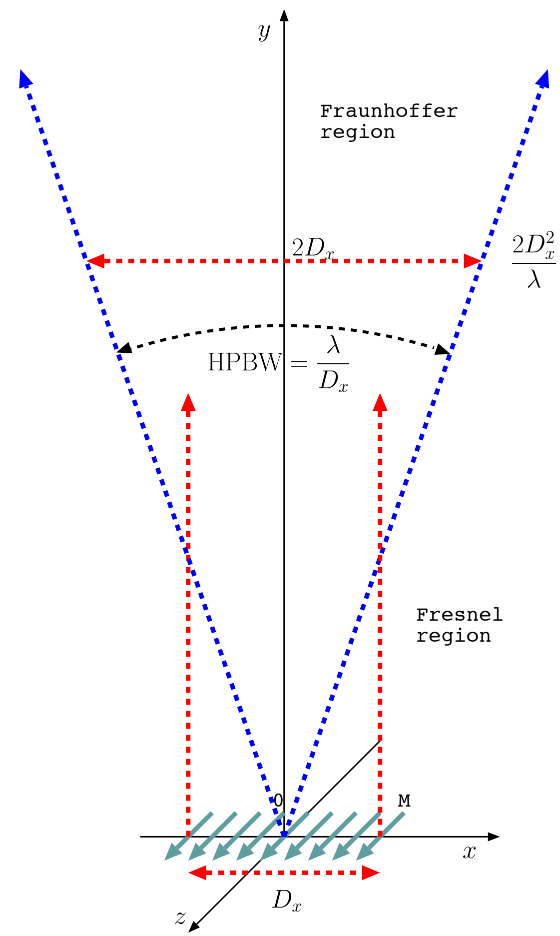

- Consider now an N-element broadside array (like the one just considered) having a far-field gain function (from Lecture 12)

$$G(\theta,\phi) = D\sin^2\theta \frac{\sin^2(\frac{N}{2}kd\sin\theta\cos\phi)}{N^2\sin^2(\frac{1}{2}kd\sin\theta\cos\phi)}.$$

The array gain

$$G(90^\circ,\phi) = D\frac{\sin^2(\frac{N}{2}kd\cos\phi)}{N^2\sin^2(\frac{1}{2}kd\cos\phi)}$$

on $\theta = 90^\circ$ has its "first nulls" around the mainlobe at angles ϕ, or $\gamma \equiv 90^\circ - \phi$, satisfying

$$\frac{N}{2}kd\cos\phi = \frac{2\pi/\lambda}{2}\underbrace{Nd}_{D_x}\sin\gamma = \pm\pi \quad \Rightarrow \quad D_x\sin\gamma = \pm\lambda,$$

so that "beam-width between first nulls" is

$$\text{BWFN} = 2|\gamma| \approx \frac{2\lambda}{D_x}$$

for $D_x \gg \lambda$.

- Approximately speaking, the "half-power beam width" between the points of $D/2$ in the gain-pattern works out to be

$$\text{HPBW} \approx \frac{1}{2}\text{BWFN} = \frac{\lambda}{D_x}$$

in radian units.

- Multiplying the HPBW with the Rayleigh distance we find that

$$\text{HPBW} \times \frac{2D_x^2}{\lambda} = \frac{\lambda}{D_x} \times \frac{2D_x^2}{\lambda} = 2D_x,$$

which indicates that at the border of Fraunhoffer region the "antenna beam" between its half-power points is about twice as wide in the transverse direction as the physical size of the array, as shown in the cartoon in the margin. This is a "physical picture" that should be kept in mind (and can be easily extrapolated into Fresnel and Fraunhoffer regions when needed).

  - Note that increasing the array size D_x causes:
    1. A larger Rayleigh distance,
    2. A thicker column of radiation field in Fresnel region,
    3. A narrower HPBW in Fraunhoffer region.

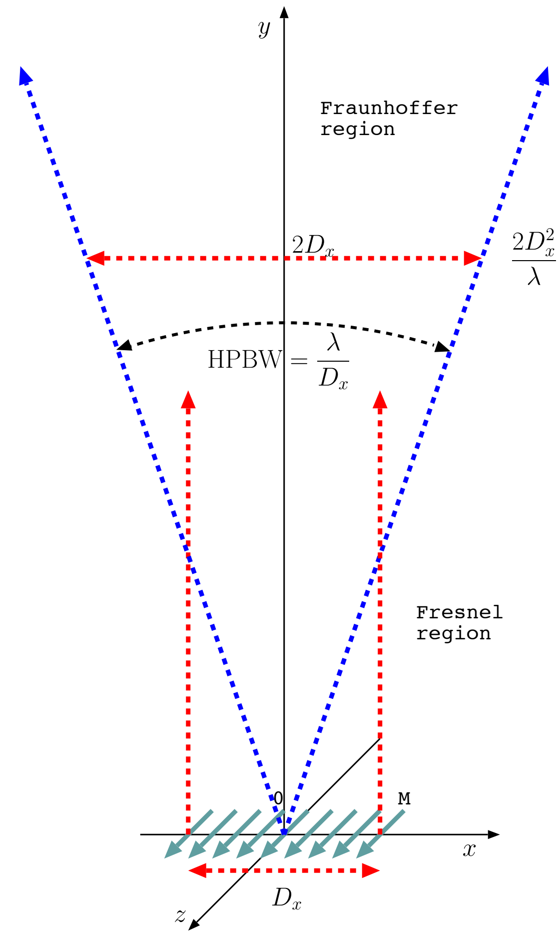

The inverse relation between antenna size D_x and the HPBW, that can be summarized as

$$\text{HPBW} \times D_x = \lambda,$$

is reminiscent of "uncertainty relation" from quantum mechanics as well as the relation between bandwidth and impulse response length of filter circuits — underlying all such relationships is of course a Fourier transform pair (between frequency response and impulse response in filter circuits; between momentum and position wave functions in quantum mechanics; between effective length function and spatial current distribution in antennas).

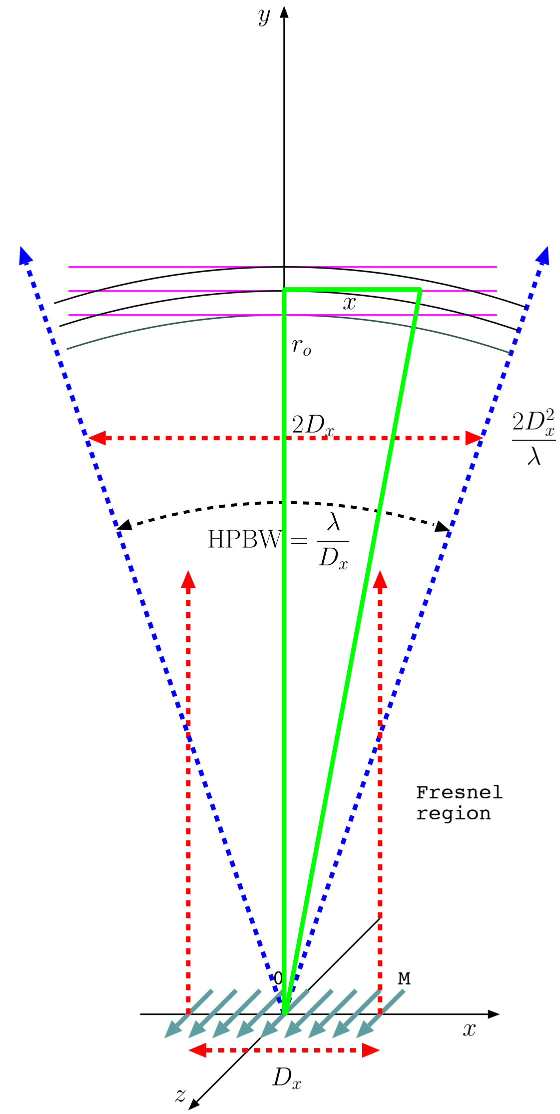

- In the Fraunhoffer region, we can express the radiation field of a $\hat{z}$-polarized antenna or antenna array as

$$\tilde{\mathbf{E}}(\mathbf{r}) = j\eta_o I_o k \ell_{eff}(\theta, \phi) \sin\theta \frac{e^{-jkr}}{4\pi r}\hat{\theta}.$$

  - This "globally" spherical-wave field can be considered a plane-wave field "locally" in any neighborhood of

$$\mathbf{r} = \mathbf{r}_o \equiv (x_o, y_o, z_o) = (r_o, \theta_o, \phi_o)$$

    within the Fraunhoffer region.
  - The expression for plane-wave approximation in the neighborhood of $\mathbf{r} = \mathbf{r}_o$ is simply

$$\tilde{\mathbf{E}}_p(\mathbf{r}) \equiv j\eta_o I_o k \ell_{eff}(\theta_o, \phi_o) \sin\theta_o \frac{e^{-jk\hat{r}_o \cdot \mathbf{r}}}{4\pi r_o}\hat{\theta}_o,$$

    where

$$\hat{r}_o \equiv \frac{\mathbf{r}_o}{|\mathbf{r}_o|}.$$

This phasor expression, that approximates the spherical wave phasor in the neighborhood of $\mathbf{r} = \mathbf{r}_o$, and is identical to $\tilde{\mathbf{E}}(\mathbf{r})$ at $\mathbf{r} = \mathbf{r}_o$, is recognized as a *plane wave* because it has the same numerical value (as a complex vector) on *planes* of constant phase defined by

$$k\hat{r}_o \cdot \mathbf{r} = \text{const.}$$

perpendicular to unit vector $\hat{r}_o$. This is a plane wave propagating in direction $\hat{r}_o$ and is *assigned* a **wave vector**

$$\mathbf{k} = k\hat{r}_o.$$

More on the *wave vector* concept later on...

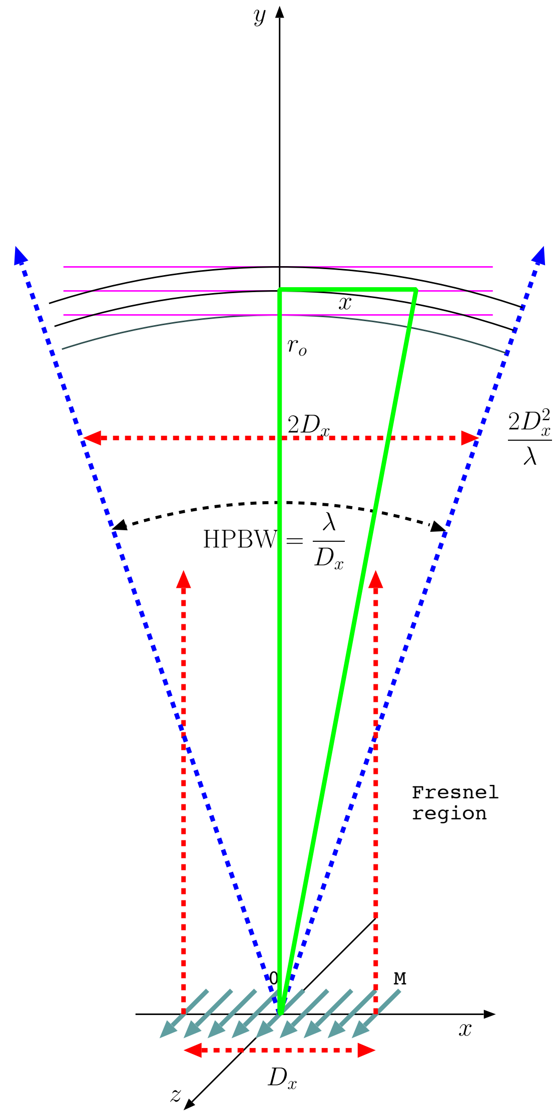

- Notice that the plane-wave field $\tilde{\mathbf{E}}_p(\mathbf{r})$ can also be expressed more compactly as

$$\tilde{\mathbf{E}}_p(\mathbf{r}) = \hat{\theta}_o |\tilde{\mathbf{E}}(\mathbf{r}_o)| e^{-jk\hat{r}_o \cdot \mathbf{r}},$$

  disregarding a possible phase offset (position independent) equal to the angle of $jI_o\ell_{eff}(\theta_o, \phi_o)$.

- The deviation of this plane-wave field from the spherical-wave field $\tilde{\mathbf{E}}(\mathbf{r})$, as $\mathbf{r}$ departs from $\mathbf{r}_o$, will be dominated by the *discrepancies* in phase variations of $\tilde{\mathbf{E}}(\mathbf{r})$ and $\tilde{\mathbf{E}}_p(\mathbf{r})$, rather than the much slower variation of $|\tilde{\mathbf{E}}(\mathbf{r})|$ with respect to $|\tilde{\mathbf{E}}_p(\mathbf{r})|$.

  That is, the **wave-front curvature** of spherical $\tilde{\mathbf{E}}(\mathbf{r})$ will be the main cause of the differences that emerge between $\tilde{\mathbf{E}}(\mathbf{r})$ and $\tilde{\mathbf{E}}_p(\mathbf{r})$ as $\mathbf{r}$ departs from $\mathbf{r}_o$.

We next determine the size of a region around $\mathbf{r} = \mathbf{r}_o$ where this wave-front curvature can be neglected. Our criterion will be to keep the phase discrepancy between $\tilde{\mathbf{E}}(\mathbf{r})$ and $\tilde{\mathbf{E}}_p(\mathbf{r})$ due to wave front curvature sufficiently small.

- For simplicity, let

$$\mathbf{r}_o = r_o\hat{y}$$

and compare the phase delay of phasors$\tilde{\mathbf{E}}_p(\mathbf{r})$ and $\tilde{\mathbf{E}}(\mathbf{r})$ at $\mathbf{r} = \mathbf{r}_o + \hat{x}x$.

  – The phase delay of $\tilde{\mathbf{E}}_p(\mathbf{r})$ at $\mathbf{r} = \mathbf{r}_o + \hat{x}x$ is

$$\Phi_p = kr_o$$

  since $\mathbf{r}_o + \hat{x}x$ and $\mathbf{r}_o$ reside on the same constant phase plane of $\tilde{\mathbf{E}}_p(\mathbf{r})$ (see margin).

  – The phase delay of $\tilde{\mathbf{E}}(\mathbf{r})$ at $\mathbf{r} = \mathbf{r}_o + \hat{x}x$ is

$$\Phi = k|r_o\hat{y} + x\hat{x}| = k\sqrt{r_o^2 + x^2}.$$

  – The phase discrepancy between $\tilde{\mathbf{E}}_p(\mathbf{r})$ and $\tilde{\mathbf{E}}(\mathbf{r})$ at $\mathbf{r} = \mathbf{r}_o + \hat{x}x$ because of wave front curvature is then

$$\begin{aligned}\Delta\Phi &= \Phi - \Phi_p = k\sqrt{r_o^2 + x^2} - kr_o = k(\sqrt{r_o^2 + x^2} - r_o) \\ &\approx kr_o(1 + \frac{1}{2}\frac{x^2}{r_o^2} - 1) = \frac{2\pi}{\lambda}\frac{x^2}{2r_o} = \frac{\pi}{4}\frac{(2x)^2}{\lambda r_o}\end{aligned}$$

  using the first two terms of the binomial expansion of $\sqrt{1 + \frac{x^2}{r_o^2}}$.

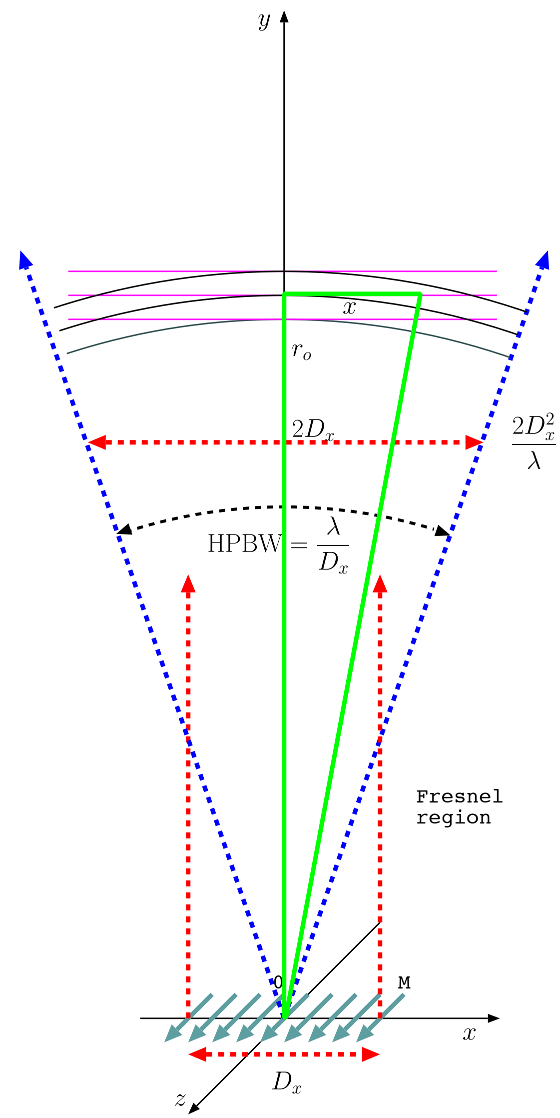

– Clearly then, if we were to take

$$\frac{(2x)^2}{\lambda r_o} \ll 1 \quad \Leftrightarrow \quad 2x < \sqrt{\lambda r_o} \text{ then we would have } \Delta\Phi \ll \frac{\pi}{4} \text{ rad.}$$

Thus, plane-wave approximation of a spherical wave about position $\mathbf{r}_o$ will have negligible errors within a box with dimensions less than $\sqrt{\lambda r_o}$ known as Fresnel distance.

– Note that Fresnel distance measuring the size of the region where plane wave approximation is acceptable grows as the square root of r_o. Smallest meaningful value of Fresnel distance is for

$$r_o = \frac{2D_x^2}{\lambda} \text{ (Rayleigh distance)}$$

in which case

$$\text{Fresnel distance} = \sqrt{\lambda r_o} = \sqrt{2}D_x.$$

An antenna beam is always (at all $|\mathbf{r}_o|$) broader than a Fresnel distance and thus only portions of an antenna beam can be well represented by a plane wave. A superposition of many (infinite) plane waves would be required for an accurate representation of an entire beam.

Example: For $\lambda = 10$ m (30 MHz) and $r_o = 100$ km, we have $\sqrt{\lambda r_o} = 1$ km. So at a distance of 100 km away from an HF source the wave field looks planar over a neighborhood of about less than a km in extent (or about 100 wavelengths).